EFFECTS OF POSITIONAL INFORMATION TIME LAGS ON AUTONOMOUS VEHICLE GUIDANCE AND CONTROL

Fotis A. Papoulias, Daniel V. Venne and George P. Cummings

Naval Postgraduate School, Department of Mechanical Engineering,
Monterey, CA 93943, U.S.A.

Int. Shipbuild. Progr., **41**, no. 428 (1994) pp. 361-392

Received: October 1993
Accepted: June 1994

The problem of loss of stability of autonomous vehicles maneuvering in the horizontal plane is considered. Path keeping is achieved through linear full state feedback for orientation control, pure pursuit guidance, and either zero or first order memory holds for navigational information. Stability maps are generated parametrized in terms of navigational time lag, guidance visibility distance, and control time constant. Nonlinear bifurcation analysis is conducted which reveals the occurence of both supercritical and subcritical Hopf bifurcations to periodic solutions. The results can be used in design to guarantee stability under finite disturbances for a given vehicle system equipped with separate navigation, guidance, and control functions.

Nomenclatuur

d	guidance law visibility distance
d_0	critical visibility distance for $T = 0$
d_T, d_1	critical visibility distance for $T \neq 0$
d_2	critical visibility distance for two point formula
δ	rudder angle deflection
δ_{sat}	saturation limit of δ
K	nonlinear stability coefficient
k_1, k_2, k_3	heading angle, sway velocity, and turning rate control gains
N	yaw moment
r	yaw rate
t_c	control time constant
T	positional information time lag
u	surge velocity
v	sway velocity
y	lateral position

Y	sway force
ψ	heading angle
ψ_c	commanded heading angle

1. Introduction

Autonomous vehicles suitable for use in modern applications require high maneuverability, quick reponse, and robust performance characteristics [Healey *et al.* (1992)]. In order to maintain accurate track keeping characteristics, a suitable combination of path planning, navigation, guidance, and crontrol design is needed [Papoulias (1991)]. Sufficient information is obtained from charted obstacles and the environment for smooth paths to be generated for the vehicle to follow [Kanayama & Hartman (1989)]. Although it is possible to design a nonlinear controller which incorporates and utilizes information on the nonlinear dynamic properties of the vehicle, as well as the geometric nonlinearities of the desired track, the resulting scheme tends to be very complex and time consuming [Cottle (1993)]. The alternative is to use separated navigation, guidance, and autopilot functions. A certain level of feedback is provided at the navigation level trough the use of sonars in order to replan a path when uncharted obstacles or when the mission objectives have changed. This operation is event-driven and occurs asynchronously, and in most cases it does not affect stability and performance of the overall navigation, guidance, and control scheme. Based on the provided navigational information, the guidance law generates heading commands, which are executed by the control law by appropriate use of the vehicle effectors, such as control surfaces and cross body thrusters. However, the time required to process sonar data and/or inertial positional information may be significant and can not be neglected [Kwak *et al.* (1992)]. In addition, the guidance and control laws must be as fast as possible in order to ensure accurate path keeping characteristics. The navigational positional information time lags, as well as the dynamic lags due to the vehicle inertia, however, set a limit on the vehicle reaction time. therefore, stability of the combined scheme becomes an issue that needs to be analyzed.

Previous studies have established stability boundaries for guidance and control laws in horizontal [Papoulias (1991)] and vertical plan [Papoulias (1993)] maneuvering along straight line paths, as well as curved segments [Papoulias (1992)]. The most important assumption in those results was the existence of instantaneous positional information updates when needed. In this work we relax the latter assumption. Stability boundaries are computed parametrized by the amount of positional information time lag. Results are presented based on eigenvalue and frequency response techniques. Linear stability analysis predicts the shape of the stability boundaries, while vehicle motions in the vicinity of the corresponding boundary are assessed using nonlinear bifurcation theory [Guckenheimer &

Holmes (1983)]. It is shown that loss of stability occurs as generic Hopf bifurcations, where upon loss of stability of straight line motion a family of periodic solutions appears. Nonlinear expansions utilizing center manifold approximations and integral averaging techniques, reveal that these Hopf bifurcations can occur either in supercritical or subcritical forms. In the supercritical case, a stable family of limit cycles is generated immediately after the nominal motion becomes unstable. In the subcritical case, however, the resulting limit cycles are initially unstable and they are generated even before the nominal motion loses its stability. In the latter case, the domain of convergence of straight line motion becomes increasingly smaller as the stability boundary is reached. As a result, the methods developed in this work characterize the degree of confidence of the computed stability boundaries by examining stability under finite external disturbances. All computations are performed for the Naval Postgraduate School autonomous underwater vehicle for which a set of geometric properties and slow motion hydrodynamic derivatives is available [Bahrke (1992)]. Unless otherwise mentioned, all results are presented in standard nondimensional form, with respect to the vehicle length, 2.2 m, and nominal forward speed, 0.6 m/sec.

2. Problem formulation

2.1. Equations of motion

Restricting our attention to motion in the horizontal plane, the mathematical model consists of the nonlinear sway and yaw equations of motion. In a moving coordinate frame fixed at the vehicle's geometric center, Newton's equations of motion are,

$$m(\dot{v} + ur + x_G\dot{r}) = Y, \tag{1}$$

$$I_z\dot{r} + mx_G(\dot{v} + ur) = N, \tag{2}$$

where v and r the relative sway and yaw velocities of the moving vehicle with respect to the water, m is the vehicle mass, x_G is the longitudinal position of the center of gravity, and Y, N represent the total excitation sway force and yaw moment, respectively. These forces can be expressed as the sum of quadratic drag terms and first order memoryless polynomials in v and r. The latter represents the hydrodynamic added mass and damping at some representative low frequency of motion. In this way, Y and N can be expressed as,

$$Y = \frac{1}{2}\varrho l^4 Y_{\dot{r}}\dot{r} + \frac{1}{2}\varrho l^3(Y_{\dot{v}}\dot{v} + Y_r ur) + \frac{1}{2}\varrho l^2 Y_v uv$$

$$- \frac{1}{2}\varrho \int_{\text{stern}}^{\text{bow}} C_D(\xi)h(\xi)\frac{(v + \xi r)^3}{|v + \xi r|}\,d\xi + \frac{1}{2}\varrho l^2 Y\delta u^2\delta, \tag{3}$$

$$N = \frac{1}{2}\varrho l^5 Y_{\dot{r}}\dot{r} + \frac{1}{2}\varrho l^4(N_{\dot{v}}\dot{v} + N_r ur) + \frac{1}{2}\varrho l^3 N_v uv$$

$$- \frac{1}{2}\varrho \int_{\text{stern}}^{\text{bow}} C_D(\xi)h(\xi)\frac{(v + \xi r)^3}{|v + \xi r|}\,d\xi + \frac{1}{2}\varrho l^3 N\delta u^2\delta, \tag{4}$$

where l is the vehicle length, Y_a and N_a represent partial derivatives of Y and N with respect to the indicated variable a, C_D is the local drag coefficient at some location ξ along the length of the hull, $h(\xi)$ is the local vehicle height at the same location, and δ is the effective rudder angle.

Equations (1) and (2) can be nodimensionalized with respect to the constant forward speed u, and the vehicle length l; the dimensionless time variable is tu/l. The cross flow integral drag terms become important for hovering operations or low speed maneuvering, whereas at relatively low angles of attack with respect to the water, the steering response is predominantly linear. Therefore, we can neglect these quadratic drag terms for the analysis that follows, numerical experience shows that the induced error is very small and does not affect the salient qualitative features of our results. This assumption has been extensively verified in experiments, where it has been observed that quadratic drag needs to be incorporated in the modeling of the vehicle only at zero speed hovering and sideways positioning.

The model becomes complete with the addition of the expressions for the vehicle yaw rate,

$$\dot{\psi} = r, \tag{5}$$

and the inertial position rate,

$$\dot{y} = u\sin\psi + v\cos\psi, \tag{6}$$

where ψ is the vehicle heading angle. A standard inertial (x,y) system is introduced here where the x-axis points in the assumed nominal straight line path, and the y-axis is distance from the reference path.

2.2. Navigation, guidance and control

Steering control is based on the linearized set of equations (1) through (5), which is written in the form,

$$\dot{\upsilon} = r,$$

$$\dot{v} = a_{11}uv + a_{12}ur + b_1u^2\delta,$$

$$\dot{r} = a_{21}uv + a_{22}ur + b_2u^2\delta, \tag{7}$$

where the coefficients a_{ij}, b_i are functions of the vehicle hydrodynamic coefficients and geometric properties. Linear full state feedback, [Friedland (1986)], can be introduced in the form,

$$\delta = k_1(\psi - \psi_c) + k_2v + k_3r, \tag{8}$$

where ψ_c is the commanded heading angle which is a function of the guidance law characteristics as seen later in this section. The feedback gains k_1, k_2, k_3 are computed such that the closed loop system (7) and (8) has the desired dynamics, in linearized sense. The existence of the difference $(\psi - \psi_c)$ in the control law (8) has the effect of trying to point the vehicle's longitudinal axis towards the desired heading. It is reminded that the commanded straight line path is assumed to lie along the earth-fixed x-axis. More general paths can be adequately discretized into a series of leading straight line segments [Papoulias & Chism (1992)].

If the desired characteristic equation is selected so that its time constant is t_c dimensionless seconds, its general form becomes,

$$\lambda^3 + \alpha_1\lambda^2 + \alpha_2\lambda + \alpha_3 = 0, \tag{9}$$

where,

$$\alpha_1 = \frac{3}{t_c}, \quad \alpha_2 = \frac{3}{t_c^2}, \quad \alpha_3 = \frac{1}{t_c^3}.$$

The controller gains are computed by equating the coefficients of the desired and actual characteristic equations as,

$$(b_2a_{11} - b_1a_{21})u^3k_1 = \alpha_3,$$

$$(b_1a_{22} - b_2a_{12})u^3k_2 + (b_2a_{11} - b_1a_{21})u^3k_3 = \alpha_2 + b_2u^2k_1 - (a_{11}a_{22} - a_{12}a_{21})u^2,$$

$$b_1u^2k_2 + b_2u^2k_3 = -\alpha_1 - (a_{11} + a_{22})u. \tag{10}$$

Due to the explicit dependence on u, the gains k_1, k_2, k_3 are continuously updated for different nominal forward speeds.

A guidance law is needed to provide the appropriate commanded heading angle ψ_c in (8). Such a typical orientation guidance law is based on the line of sight angle, between the vehicle longitudinal axis and a moving reference point located ahead of the vehicle at a constant distance, d, along the commanded straight line path. The simplest law is when the commanded heading equals precisely this line of sight angle,

$$\psi_c = -\tan^{-1}\frac{y}{d}. \tag{11}$$

The distance d in (11) is referred to as the lookahead or visibility distance. Finally, the positional error information, y, needed in (11) is provided by the navigation function, which in this work is assumed to provide the exact estimate of y with a time lag of T dimensionless seconds. Therefore,

$$y = y(t - T), \tag{12}$$

in (11). the time lag, T, models the necessary time to process sonar range information and thereby reconstruct an accurate representation of the environment. Equations (12) and (11) substituted back into (8) provide the combined navigation, guidance, and control model used in this work. It should be pointed out that in order to capture the effect of rudder angle saturation, we re-write (8) in the form,

$$\delta = \delta_{sat}\tan\ h\left[\frac{k_1(\psi - \psi_c) + k_2v + k_3r}{\delta_{sat}}\right], \tag{13}$$

where δ_{sat} is the saturation limit of δ, typically set at ± 0.4 radians. Equation (13) produces the same slope at zero as (8), and it provides a smooth representation of the nonlinear saturation function which is required by the analysis that is presented in the following sections. Rudder saturation is a feature that is introduced in the system to prevent rudder stall at higher angles of attack. Although some stall of the forward rudder has been observed in certain experiments, most of the time it can be neglected. We also assume that rudder response is instantaneous. This is be-

cause the DC-servos that control the vehicle control surfaces have considerable smaller time constants than the dominant vehicle turning dynamics.

3. Stability analysis

3.1. Eigenvalue analysis

The linearized navigation, guidance, and control equations of motion ar written as,

$$\dot{\psi} = r, \tag{14}$$

$$\dot{v} = b_1u^2k_1\psi + (a_{11} + b_1uk_2)uv + (a_{12} + b_1uk_3)ur + b_1u^2\frac{k_1}{d}y(t - T), \tag{15}$$

$$\dot{r} = b_2u^2k_1\psi + (a_{21} + b_2uk_2)uv + (a_{22} + b_2uk_3)ur + b_2u^2\frac{k_1}{d}y(t - T), \tag{16}$$

$$\dot{y} = u\psi + v. \tag{17}$$

The system of equations (14) through (17) represents an infinite dimensional vector field, since the time delay operator can be thought of in terms of its Taylor series,

$$y(t - T) = y - T\dot{y} + \frac{T^2}{2}\ddot{y} - \frac{T^3}{6}y^{(iii)} + \ldots \tag{18}$$

Practical computations can be performed by truncating (18) to first, second, or third order.

A first order approximation in the time lag T is achieved by,

$$y(t - T) = y - T\dot{y}, \quad \text{or} \quad y(t - T) = y - T(u\psi + v). \tag{19}$$

Substitution of (19) into (15) and (16) yields,

$$\begin{bmatrix} \dot{\psi} \\ \dot{v} \\ \dot{r} \\ \dot{y} \end{bmatrix} = \begin{bmatrix} 0 & 0 & 1 & 0 \\ A_{21,1} & A_{22,1} & A_{23,1} & A_{24,1} \\ A_{31,1} & A_{32,1} & A_{33,1} & A_{34,1} \\ u & 1 & 0 & 0 \end{bmatrix} \begin{bmatrix} \psi \\ v \\ r \\ y \end{bmatrix}, \tag{20}$$

where the entries $A_{ij,1}$ are shown in the Appendix. The standard eigenvalue problem (20) can be solved numerically in order to establish stability or instability of

straight line motion. In general, we expect that for a given time lag T and control time constant t_c, there must be a minimum required visibility distance d for stability. Convergence to the nominal motion should then be ensured, in a linear sense, for values of d greater than its critical value.

A second order approximation in T is achieved by,

$$y(t - T) = y - T\dot{y} + \frac{T^2}{2}\ddot{y} = y - T(u\psi + v) + \frac{T^2}{2}(ur + \dot{v}). \tag{21}$$

Substitution of (21) into (15) and (16) yields,

$$\begin{bmatrix} \dot{\psi} \\ \dot{v} \\ \dot{r} \\ \dot{y} \end{bmatrix} = \begin{bmatrix} 0 & 0 & 1 & 0 \\ A_{21,2} & A_{22,2} & A_{23,2} & A_{24,2} \\ A_{31,2} & A_{32,2} & A_{33,2} & A_{34,2} \\ u & 1 & 0 & 0 \end{bmatrix} \begin{bmatrix} \psi \\ v \\ r \\ y \end{bmatrix}, \tag{20}$$

where the elements $A_{ij,2}$ are also included in the Appendix. Solution to the eigenvalue problem (22) provides a more accurate approximation to the stability domain.

Finally, a third order approximation in T is based on,

$$y(t - T) = y - T\dot{y} + \frac{T^2}{2}\ddot{y} - \frac{T^3}{6}u^{(iii)}. \tag{23}$$

Similar algebraic steps as in the previous two approximations result in the following generalized eigenvalue problem,

$$\begin{bmatrix} 1 & 0 & 0 & 0 & 0 \\ 0 & 1 & 0 & 0 & 0 \\ 0 & 0 & B_{33,3} & 0 & B_{35,3} \\ 0 & 0 & 0 & 1 & 0 \\ 0 & 0 & B_{53,3} & 0 & B_{55,3} \end{bmatrix} \begin{bmatrix} \dot{\psi} \\ \dot{v} \\ \dot{r} \\ \dot{y} \\ \dot{v}_2 \end{bmatrix} \begin{bmatrix} 0 & 0 & 1 & 0 & 0 \\ 0 & 0 & 0 & 0 & 1 \\ A_{31,3} & A_{32,3} & A_{33,3} & A_{34,3} & A_{35,3} \\ u & 1 & 0 & 0 & 0 \\ A_{51,3} & A_{52,3} & A_{53,3} & A_{54,3} & A_{55,3} \end{bmatrix} \begin{bmatrix} \psi \\ v_1 \\ r \\ y \\ v_2 \end{bmatrix}, \tag{24}$$

where $v_1 = v$, v_2 is the rate of change of v, and the entries of the generalized eigenvalue problem (24) are included in the Appendix. Higher order approxima-

tions in T can not produce any usable stability results, since the B-matrix in (24) becomes singular.

3.2. Comparison and normalization of results

A plot of the critical visibility distance, d_T, versus the control time constant t_c for T = 1 is shown in Figure 1, using all three approximations for y(t− T). In general, the following conclusions can be made:

1. Higher values of t_c require higher values of d in order to guarantee stability. Since higher t_c corresponds to a lower bandwidth control law, this means that a slower guidance law is needed to accomodate the slower control law.

2. Agreement between the three approximations is relatively good, the third order approximation is naturally the most accurate. The agreement is progressively better as t_c is increased. It can also be seen that, for design purposes, the first order approximation provides the most conservative estimate for the domain of stability. Since this is also the simplest to compute, we will make use of this result in the next section where we attempt to classify the dynamics of the system at the neighborhood of the stability boundary.

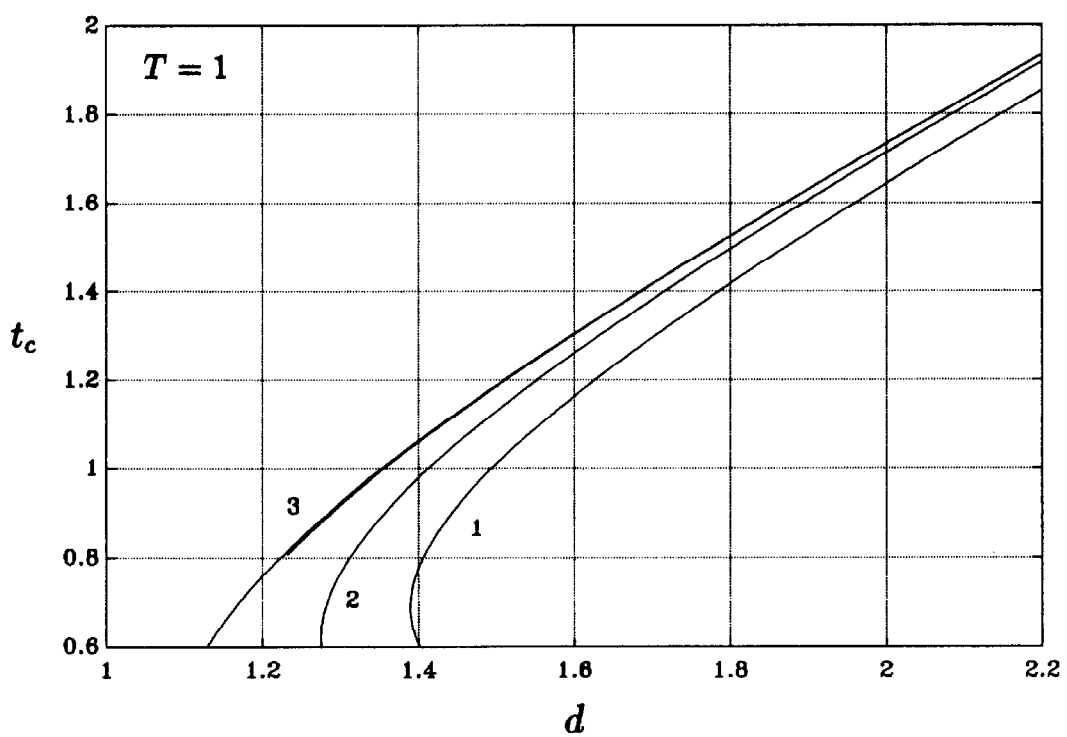

Fig. 1. Stability boundaries in the (d,t_c) parameter plane for T = 1.

For design purposes, it is desirable to normalize the results so that we can characterize the stability analysis for all values of time lag. To this end, we proceed as follows: If the vehicle side slip velocity v is very small so that it can be neglected, the vehicle equations of motion (6) and (7) take the form,

$$\dot{\psi} = r,$$

$$\dot{r} = a_{22}ur + b_2u^2\delta,$$

$$\dot{y} = u\psi. \tag{25}$$

The control law is,

$$\delta = k_1(\psi - \psi_c) + k_3r, \tag{26}$$

where the first order approximation for the commanded heading angle is employed,

$$\psi_c = \frac{y - T\dot{y}}{d}. \tag{27}$$

Based on equations (25), (26), and (27), we can get the characteristic equation of the system as,

$$\lambda^3 - (a_{22} + b_2k_3u)u\lambda^2 - b_2k_1\left(1 - u\frac{T}{d}\right)u^2\lambda - b_2k_1u^3\frac{1}{d} = 0.$$

Applying Routh's criterion to this cubic equation, we find that loss of stability occurs when,

$$(a_{22} + b_2k_3u)\left(1 - u\frac{T}{d}\right) = -\frac{1}{d},$$

from which we can get the critical visibility distance,

$$d_T = -\frac{1}{a_{22} + b_2k_3u} + Tu. \tag{28}$$

Equation (28) can be written as,

$$\frac{d^t - d_0}{T} = u, \tag{29}$$

where d_0 is the critical visibility distance for $T = 0$, and d_T the corresponding distance for $T \neq 0$. In dimensionless quantities, equation (29) is written as,

$$\frac{d_T - d_0}{T} = 1, \tag{30}$$

where d_T, d_0 are in vehicle length, and T is expressed in the time it takes to travel a vehicle length.

A comparison between the approximation expression (30), and the three Taylor series approximations (19), (21), and (23), is shown in Figure 2, for $T = 1$. As expected, the agreement if better for the first order approximation, and also for higher controller time constants t_c. This is because a high t_c results in soft vehicle response with negligible amounts of side slip. A plot of $(d_T - d_0)/T$ versus t_c using the third order approximation (23) and for different T is shown in Figure 3. As expected, the agreement increases with increasing t_c and decreasing T.

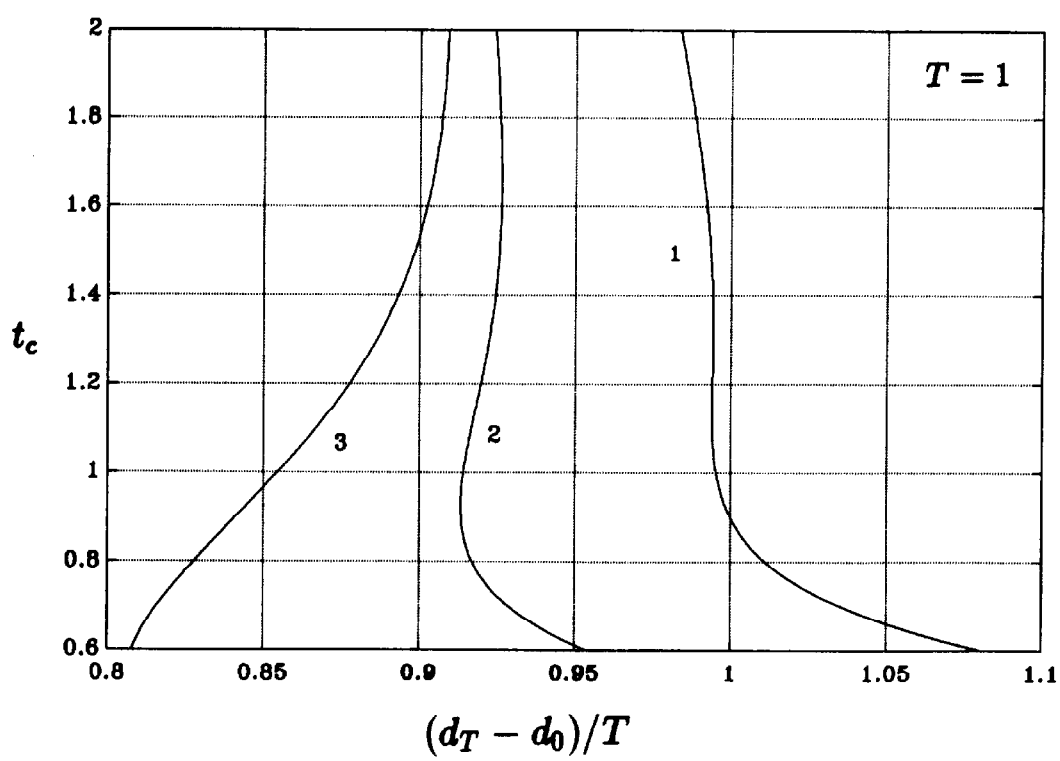

Fig. 2. Critical ratio $(d_T - d_0)/T$ versus t_c for $T = 1$, and for first, second, and third order approximations of $y(t - T)$.

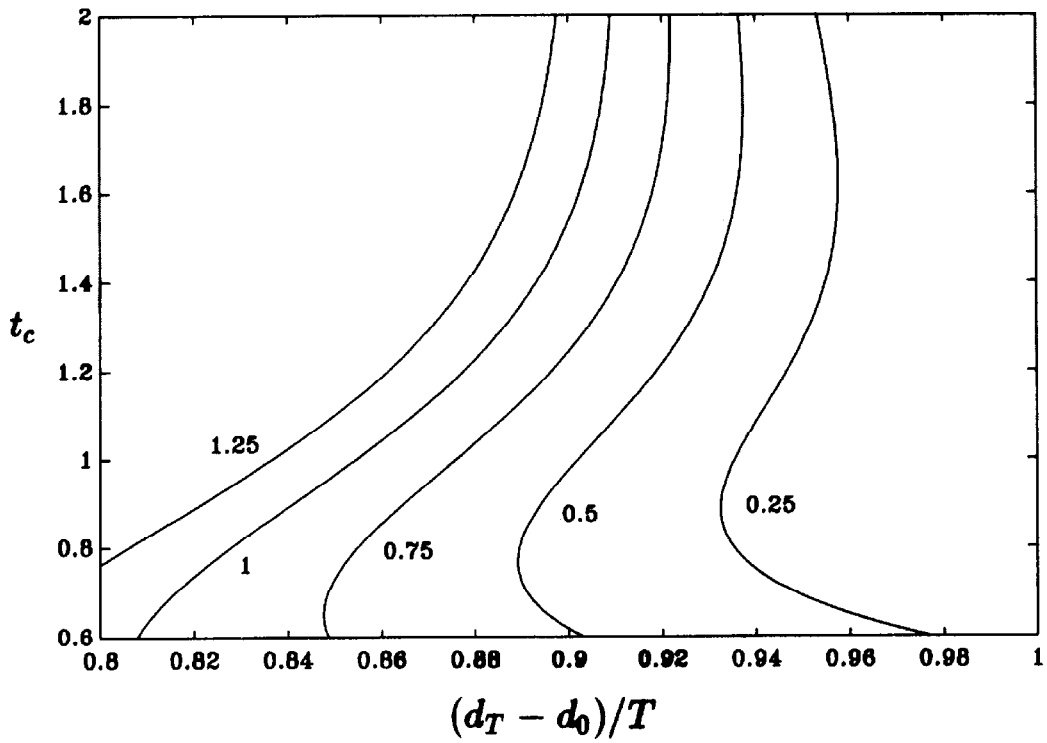

Fig. 3. Critical ratio $(d_T - d_0)/T$ versus t_c for third order approximation of $y(t - T)$, and for different values of T.

3.3. Exact computation

The previous analysis using Taylor expansions of $y(t - T)$ breaks down for approximations beyond third order, as the corresponding generalized eigenvalue problem becomes singular. A different technique should, therefore, be sought in order to obtain an exact computation of the stability curves and check the validity of our calculations. This technique is based on frequency response methods and it utilizes Nyquist's criterion for stability [Friedland (1986)]. We write the equations of motion (14) through (17) in the Laplace domain, where,

$$y(t - T) \rightarrow ye^{-Ts}, \tag{31}$$

is the time delay operator. The characteristic equation of the system is,

$$s^4 + \alpha_1 s^3 + \alpha_2 s^2 + \alpha_3 s + (\beta_2 s^2 + \beta_1 s + \beta_0)\alpha_3 \frac{1}{d} e^{-ts} = 0, \tag{32}$$

where,

$$\beta_0 = u,$$

$$\beta_1 = -\frac{a_{12}b_2 - a_{22}b_1 + b_2}{b_2a_{11} - b_1a_{21}},$$

$$\beta_2 = -\frac{b_1}{u(b_2a_{11} - b_1a_{21})},$$

and α_1, α_2, α_3 are given in terms of t_c in (9). The characteristic equation (32) is written as,

$$1 + \frac{1}{d}G(s) = 0, \tag{33}$$

where,

$$G(s) = \frac{(\beta_2 s^2 + \beta_1 s + \beta_0)\alpha_3 e^{-Ts}}{s(s^3 + \alpha_1 s^2 + \alpha_2 s + \alpha_3)}, \tag{34}$$

is the open loop transfer function, and 1/d denotes the effective position gain. For stability, we can utilize the Nyquist criterion which states that the critical value d_T can be computed from,

$$\frac{1}{d}|G(j\omega)| = 1 \qquad \text{for} \qquad \arg\{G(g\omega)\} = -\pi, \tag{35}$$

where j denotes the imaginary unit. The argument, $\arg\{G(j\omega)\}$, of (34) is,

$$\arg\{G(j\omega)\} = -\omega T - \frac{\pi}{2} + \tan^{-1}\left(\frac{\beta_1\omega}{\beta_0 - \beta_2\omega^2}\right) - \tan^{-1}\left(\frac{\alpha_2\omega - \omega^3}{\alpha_3 - \alpha_1\omega^2}\right).$$

The two equations (35) result in the critical visibility,

$$d = \frac{\alpha_3\sqrt{(\beta_0 - \beta_2\omega^2)^2 + \beta_1^2\omega^2}}{\omega\sqrt{(\alpha_2 - \alpha_1\omega^2)^2 + (\alpha_2\omega - \omega^3)^2}}, \tag{36}$$

where ω is the solution to,

$$\frac{\beta_1\omega(\alpha_3 - \alpha_1\omega^2) - (\beta_0 - \beta_2\omega^2)(\alpha_2\omega - \omega^3)}{(\beta_0 - \beta_2\omega^2)(\alpha_3 - \alpha_1\omega^2) + \beta_1\omega(\alpha_2\omega - \omega^3)} = -\frac{1}{\tan(\omega T)}. \tag{37}$$

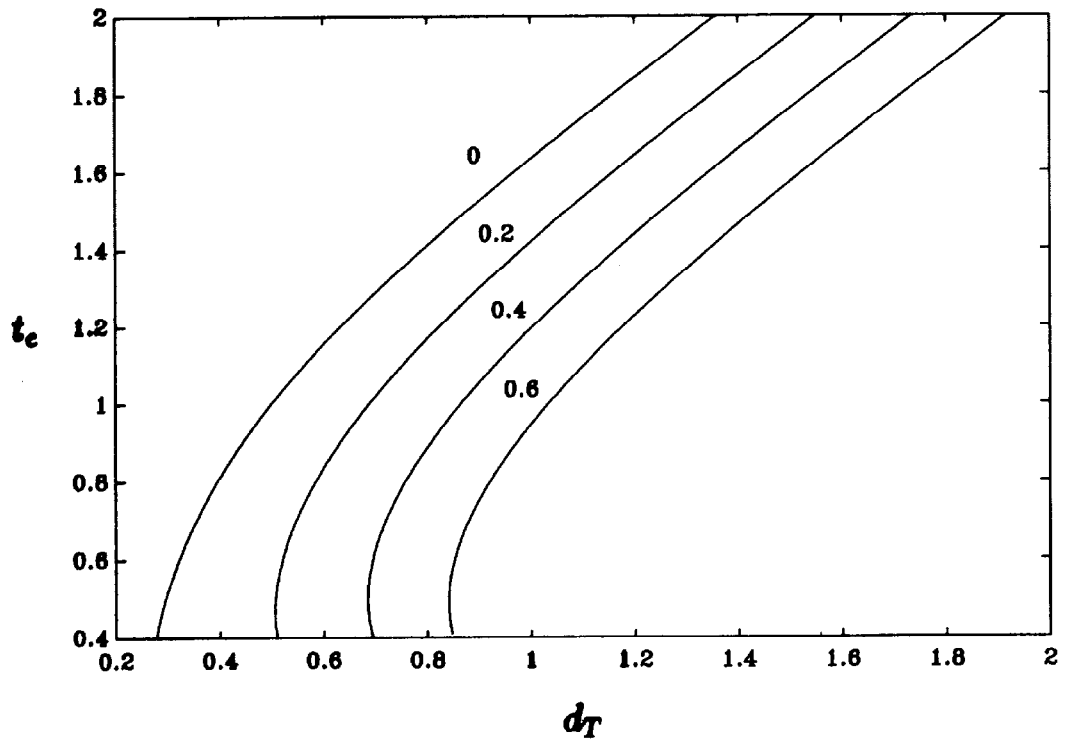

Fig. 4. Critical visibility d_T versus t_c for different values of time lag T.

Solution to (37) yields the so-called phase crossover frequency, and then the critical value of d, d_T, is easily obtained from (36).

Typical results are presented in Figure 4 in terms of d_T versus t_c for different values of time lag T. To within the thickness of the graphs, the results are identical to those obtained using the third order Taylor series approximation (23).

4. Analysis of Hopf Bifurcation

4.1. Introduction

It can be numerically confirmed that in all cases of stability loss of the previous chapter, one pair of complex conjugate eigenvalues of the corresponding eigenvalue problem crosses transversally the imaginary axis. A situation like this in which a certain parameter is varied such that the real part of one pair of complex conjugate eigenvalues of the linearized system matrix crosses zero, results in the system leaving its steady state in an oscillatory manner. This loss of stability is called Hopf bifurcation and generically occurs in one of two ways, supercritical or subcritical. In the supercritical case, stable limit cycles are generated after the nominal straight line motion loses its stability. The amplitudes of these limit cycles are continuously increasing as the parameter distance from its critical value is increased. for small values of this criticality distance the resulting limit cycle is of small amplitude and

differs little from the initial nominal state. In the subcritical case, however, stable limit cycles are generated before the nominal state loses its stability. Therefore, depending on the initial conditions it is possible to diverge away from the nominal straight line path and converge towards a limit cycle even before the nominal motion loses its stability. This means that in the subcritical Hopf bifurcation case the domain of attraction of the nominal state is decreasing and in fact it shrinks to zero as the critical point is approached. Random external disturbances of sufficient magnitude can throw the vehicle off to an oscillatory steady state even though the nominal state may still remain stable. After the nominal state becomes unstable, a discontinuous increase in the magnitude of motions is observed as there exist no simple stable nearby attractors for the vehicle to converge to. Distinction between these two qualitatively different types of bifurcation is, therefore, essential in design. The computational procedure requires higher order approximations in the equations of motion and is the subject of the next section.

4.2. Computations

The nonlinear equations of motion are written as,

$$\dot{\psi} = r, \tag{38}$$

$$\dot{v} = a_{11}uv + a_{12}ur + b_1u^2\delta', \tag{39}$$

$$\dot{r} = a_{21}uv + a_{22}ur + b_2u^2\delta', \tag{40}$$

$$\dot{y} = u\sin\psi + v\cos\psi, \tag{41}$$

where the control law is,

$$\delta = k_1\psi + k_2v + k_3r + k_1\tan^{-1}\frac{y(t-T)}{d}, \tag{42}$$

and, including saturation,

$$\delta' = \delta_{sat}\tanh\left(\frac{\delta}{\delta_{sat}}\right). \tag{43}$$

We perform a Taylor series expansion of the equations, keeping the first non-vanishing nonlinear terms. Due to port/starboard symmetry in the problem, this means expansion to third order terms,

$$\sin\psi = \psi - \frac{1}{6}\psi^3, \qquad \cos\psi = 1 - \frac{1}{2}\psi^2, \tag{44}$$

$$\delta' = \delta - \frac{1}{3\delta_{sat}^2}\delta^3, \tag{45}$$

$$\delta = k_1\psi + k_2 v + k_3 r + \frac{k_1}{d}y(t-T) - \frac{k_1}{3d^3}y^3(t-T), \tag{46}$$

where for consistency, the term $y(t - T)$ is approximated by its first order expansion in T,

$$y(t-T) = y - T\dot{y} = y - Tu\psi + \frac{1}{6}Tu\psi^3 - Tv + \frac{1}{2}Tv\psi^2. \tag{47}$$

Substitution of equations (44) to (47) into equations (38) to (43), produces the system,

$$\dot{\mathbf{x}} = \mathbf{A}\mathbf{x} + \mathbf{g}(\mathbf{x}), \tag{48}$$

where the state variables vector is,

$$\mathbf{x} = [\psi, v, r, y]^T,$$

A is the linearized matrix at equilibrium, and $\mathbf{g}(\mathbf{x})$ contains all third order terms.

If **T** is the matrix of eigenvectors of **A** evaluated at the critical point $d = d_T$, the linear change of coordinates,

$$\mathbf{x} = \mathbf{T}\mathbf{z}, \qquad \mathbf{z} = \mathbf{T}^{-1}\mathbf{x}, \tag{49}$$

transforms system (48) into its normal coordinate form,

$$\dot{\mathbf{z}} = \mathbf{T}^{-1}\mathbf{A}\mathbf{T}\mathbf{z} + \mathbf{T}^{-1}\mathbf{g}(\mathbf{T}\mathbf{z}). \tag{50}$$

At the Hopf bifurcation point, matrix $\mathbf{T}^{-1}\mathbf{A}\mathbf{T}$ takes the form,

$$\mathbf{T}^{-1}\mathbf{A}\mathbf{T} = \begin{bmatrix} 0 & -\omega_0 & 0 & 0 \\ \omega_0 & 0 & 0 & 0 \\ 0 & 0 & p & 0 \\ 0 & 0 & 0 & q \end{bmatrix},$$

where ω_0 is the imaginary part of the critical pair of eigenvalues, and the remaining two eigenvalues p and q are negative. For values of d close to the bifurcation point d_T, matrix $\mathbf{T}^{-1}\mathbf{A}\mathbf{T}$ is,

$$\mathbf{T}^{-1}\mathbf{A}\mathbf{T} = \begin{bmatrix} \alpha'\varepsilon & -(\omega_0 + {}'\varepsilon) & 0 & 0 \\ \omega_0 + \omega'\varepsilon & \alpha'\varepsilon & 0 & 0 \\ 0 & 0 & p + p'\varepsilon & 0 \\ 0 & 0 & 0 & q + q'\varepsilon \end{bmatrix},$$

where, ε denotes the criticality difference,

$$\varepsilon = d - d_T, \tag{51}$$

ω' = derivative of the real part of the critical eigenvalues with respect to ε,
α' = derivative of the imaginary part of the critical eigenvalues with respect to ε,
p' = derivative of p with respect to ε,
q' = derivative of q with respect to ε.

Due to continuity, the eigenvalues $p + p'\varepsilon$ and $q + q'\varepsilon$ remain negative for small nonzero values of ε. Therefore, the coordinates z_3, z_4 correspond to negative eigenvalues and are asymptotically stable.

Center manifold theory predicts that the relationship between the critical coordinates z_1, z_2 and the stable coordinates z_3, z_4 is at least of quadratic order. In fact, due to the symmetry in our problem the relationship is cubic,

$$z_1 = O(z_3^3, z_4^3), \qquad z_2 = O(z_3^3, z_4^3).$$

It follows that because of this order, z_3, z_4 do not influence the third order Taylor series expansions, and can be dropped from the equations. Therefore, we can write the reduced system that describes the center manifold flow of (50) in the form,

$$\dot{z}_1 = \alpha'\varepsilon z_1 - (\omega_0 + \omega'\varepsilon)z_2 + F_1(z_1,z_2), \tag{52}$$

$$\dot{z}_2 = (\omega_0 + \omega'\varepsilon)z_1 + \alpha'\varepsilon z_2 - F_2(z_1,z_2), \tag{53}$$

where F_1, F_2 contain the third order terms,

$$F_1(z_1,z_2) = r_{11}z_1^3 + r_{12}z_1^2z_1z_2 + r_{13}z_1z_2^2 + r_{14}z_2^3, \tag{54}$$

$$F_2(z_1,z_2) = r_{21}z_1^3 + r_{22}z_1^2z_1z_2 + r_{23}z_1z_2^2 + r_{24}z_2^3, \tag{55}$$

The coefficient r_{ij} are computable from the previous Taylor expansions, see Appendix.

If we introduce polar coordinates in the form,

$$z_1 = R\cos\theta, \qquad z_2 = R\sin\theta, \tag{56}$$

we can use (52) and (53) to produce an equation describing the rate of change of the radial coordinate R,

$$\dot{R} = \alpha'\varepsilon R + P(\theta)R^3, \tag{57}$$

and a similar equation in the rate of change of the angular coordinate θ,

$$\dot{\theta} = \omega_0 + \omega'\varepsilon + Q(\theta)R^2. \tag{58}$$

The system of equations (57) and (58) contains two variables, one of which, R, is slowly varying in time, whereas the other one, θ is a fast variable. Then, equation (57) can be averaged over one cycle in θ to produce an equation with constant coefficients and similar properties,

$$\dot{R} = \alpha'\varepsilon R + KR^3, \tag{59}$$

where,

$$K = \frac{1}{2\pi}\int_0^{2\pi} P(\theta)d\theta = R\,\frac{1}{8}\,(3r_{11} + r_{13} + r_{22} + 3r_{24}). \tag{60}$$

Nontrivial equilibrium solutions of (59) correspond to limit cycles in the original system. The nontrivial equilibrium of (59), R_0, is given by,

$$R_0 = \sqrt{-\frac{\alpha'\varepsilon}{K}}\,. \tag{61}$$

In our problem, since the trivial equalibrium gains its stability for $d > d_T$, the coefficient α' is always negative. Therefore, it can be seen from (61) that a limit cycle will exist provided K and ε have the same sign. The stability properties of this limit cycle can be determined by linearization of (59) around R_0. The linearized system is,

$$\dot{R} = -2\alpha'\varepsilon(R - R_0), \tag{62}$$

and its eigenvalue is,

$$\beta = -2\alpha'\varepsilon. \tag{63}$$

We can see that the Floquet exponent (63) is negative if ε is negative, which means that K must be negative. Therefore, location and stability of limit cycles depends entirely on the cubic coefficient K which is computable from (60). We can summarize our findings as,

- If $K < 0$ then limit cycles exist for $\varepsilon < 0$ ($d < d_T$) and they are stable.
- If $K > 0$ then limit cycles exist for $\varepsilon > 0$ ($d > d_T$) and they are unstable.

4.3. Results and discussion

The cubic coefficient K is presented in Figure 5 versus the control time constant, t_c, for rudder saturation limit $\delta_{sat} = 0.4$ radians, and for different values of navigation time lag T in dimensionless seconds. It can be seen that supercritical Hopf bifurcations are ensured for t_c higher than a certain critical value. For t_c less than the critical value, the bifurcations are subcritical and higher limit cycle amplitudes are expected. The critical transition point is decreasing for increasing values of T. The range of control designs t_c for supercritical bifurcations is increasing for increasing T. This means that, although higher T requires a higher value of d for stability of straight line motion, it helps in 'softening' the response afte the initial loss of stability. Similar results can be obtained from Figure 6 which presents K versus t_c for $T = 0.4$ and for different values of δ_{sat}. As before, supercritical bifurcations are ensured for sufficiently high values of t_c, whereas the range of t_c for supercritical loss of stability is increasing with increasing available control δ_{sat}.

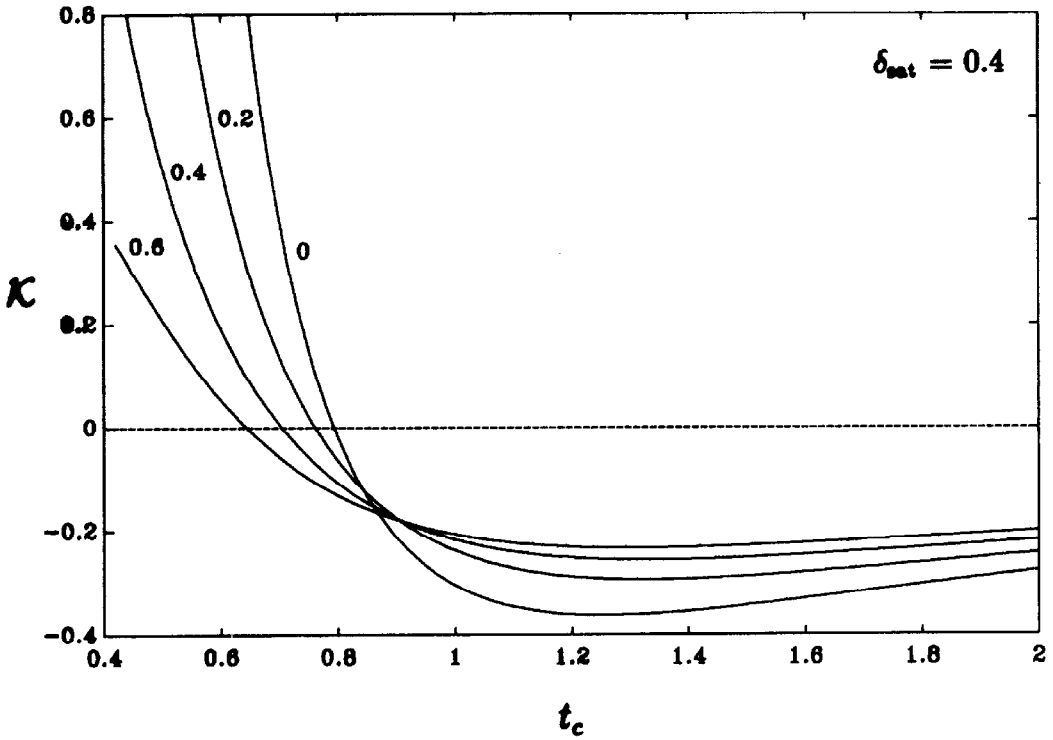

Fig. 5. Cubic coefficient K versus t_c for δ_{sat} = 0.4 and different values of T.

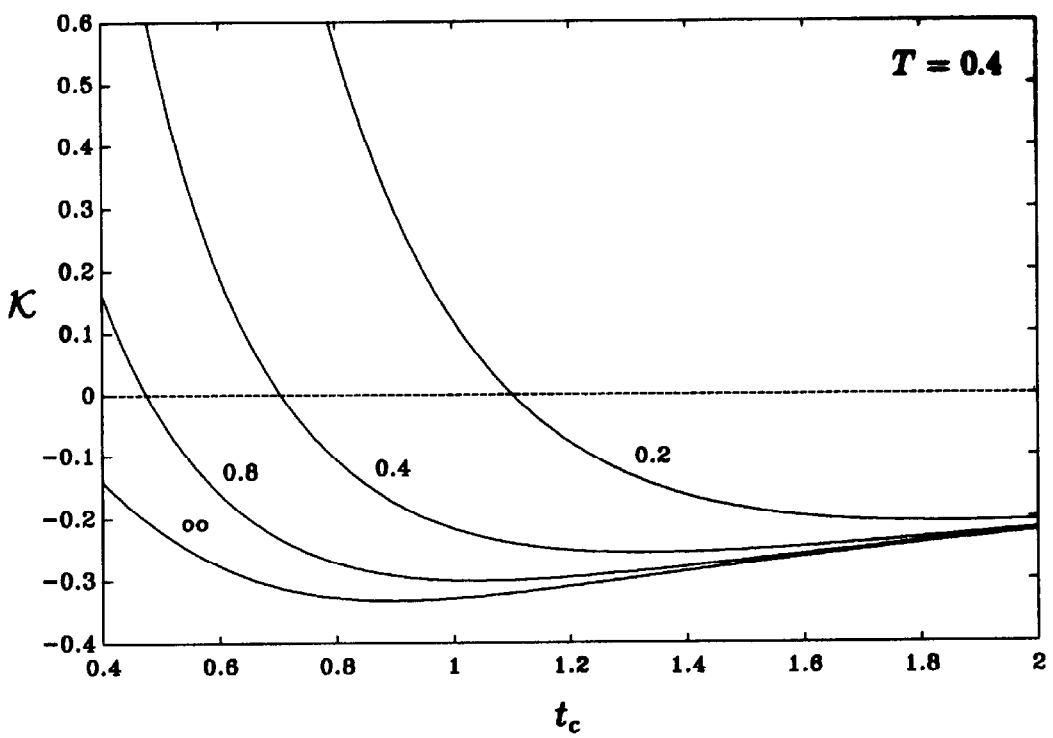

Fig. 6. Cubic coefficient K versus t_c for T = 0.4 and different values of δ_{sat}.

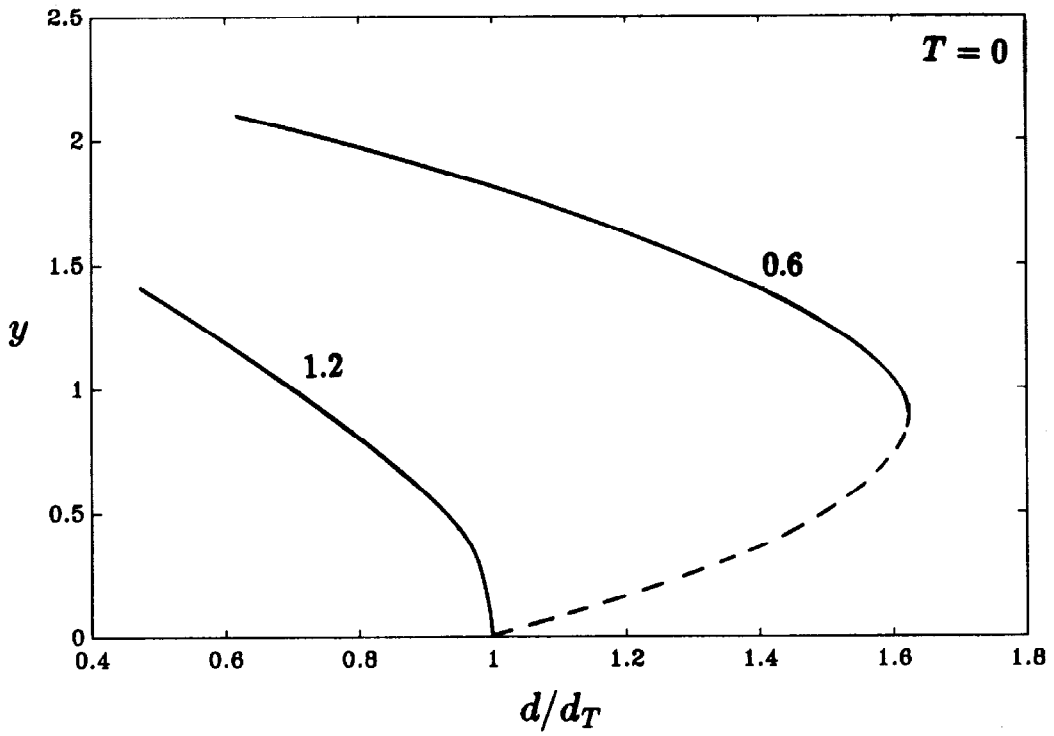

Fig. 7. Amplitudes of limit cycles versus d/d_T for $T = 0$ and two different values of t_c.

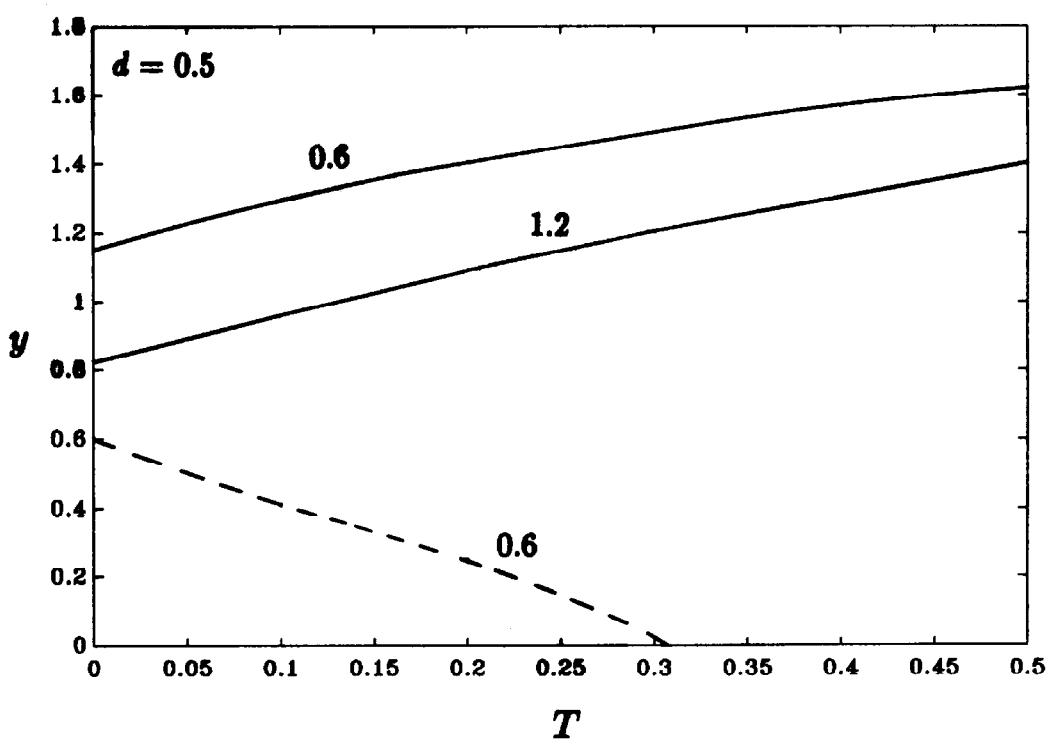

Fig. 8. Amplitudes of limit cycles versus T for $d = 0.5$ and two different values of t_c.

The theoretical results of Figures 5 and 6 are confirmed by the direct numerical integration results presented in Figures 7 and 8. Figure 7 shows limit cycle amplitudes for $T = 0$ as functions of the normalized visibility distance d/d_T. Solid curves correspond to stable limit cycles and dotted curves correspond to unstable limit cycles. The latter were numerically obtained by an iterative shooting scheme. For $t_c = 1.2$ the corresponding bifurcations are supercritical and we can observe the continuously increasing amplitudes for $d/d_T < 1$. For $t_c = 0.6$ we can observe the occurrence of unstable limit cycles for $d/d_T > 1$ characteristic of subcritical behavior. Global asymptotic stability of straight line motion appears to be possible only after exceeding the least required values of d by more than 60%. For values of d less than d_T, a discontinuous limit cycle amplitude is observed for an infinitely small initial disturbance $y \neq 0$. Figure 8 shows limit cycle amplitudes versus T for $d = 0.5$ and for the same two values of t_c. Supercritical bifurcations occur for $t_c = 1.2$ throughout the range of T, whereas for $t_c = 0.6$ supercritical bifurcations occur only for T higher than a certain critical value. Limit cycle amplitudes for the supercritical case remain consistently smaller than in the subcritical case.

5. Stability enhancement

The use of equation (12), $y = y(t - T)$, in the guidance law (11) corresponds to a zero memory navigation model: in the absence of current positional information we simply utilize the value at the previous position fix. It is possible that by expanding this to a first order memory model, the stability properties of the combined scheme will improve. To assess this we can use the previous two vehicle positions, at times $(t - 2T)$ and $(t - T)$, and extrapolate linearly to the current position. This produces the following navigational estimate,

$$y = 2y(t - T) - y(t - 2T), \tag{64}$$

which is then used in the guidance law (11).

The domain of motion stability for the two point formula (64) can be computed using a technique equivalent to Section 3.3, where the term e^{-Ts} is substituted by $2e^{-Ts} - e^{-2Ts}$. Typical results are presented in Figure 9 where the critical visibility distance, d, is plotted versus the control time constant, t_c, for $T = 0.5$, and using the two navigational formulas (12) and (64). It can be seen that in general use of the two point formula provides a larger domain of stability except for small values of t_c where the situation is reversed. Since such small values of t_c must be avoided in practice based on our analysis of Hopf bifurcations, it can be concluded that the two point formula results in stability enhancement. The critical value of t_c where use of the one point formula is preferred is generally increasing with increasing values of time lag T. This is further shown in Figure 10, where we present the ratio

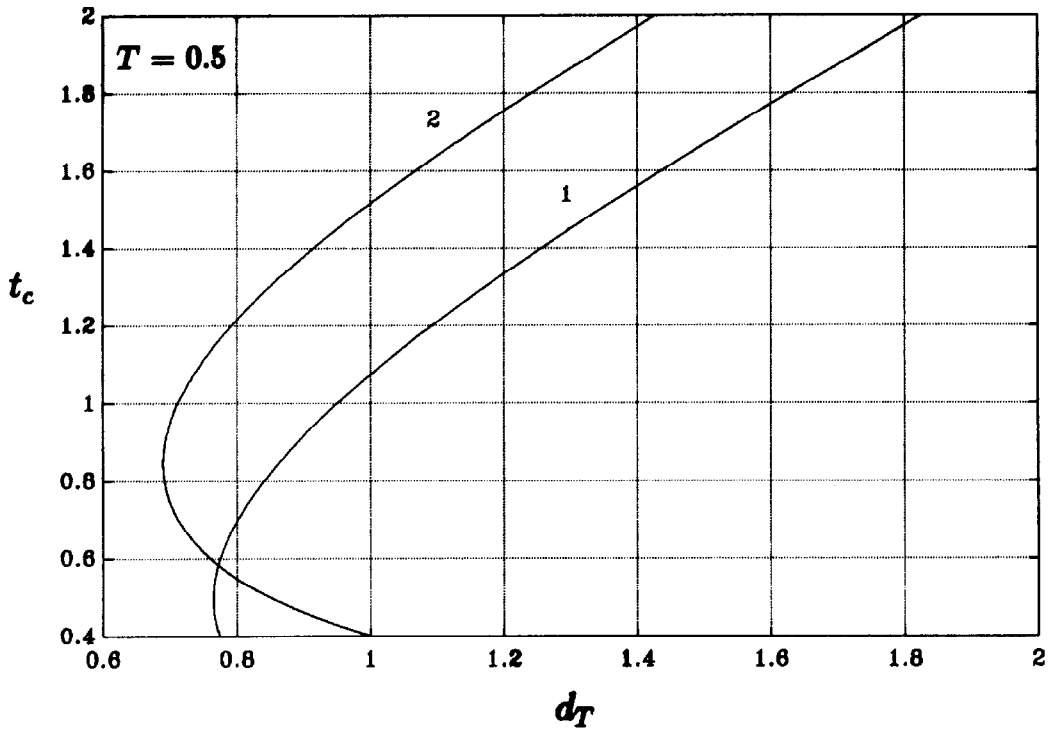

Fig. 9. Critical visibility d_T versus t_c for $T = 0.5$ using the one (1) and two (2) point navigational formulas.

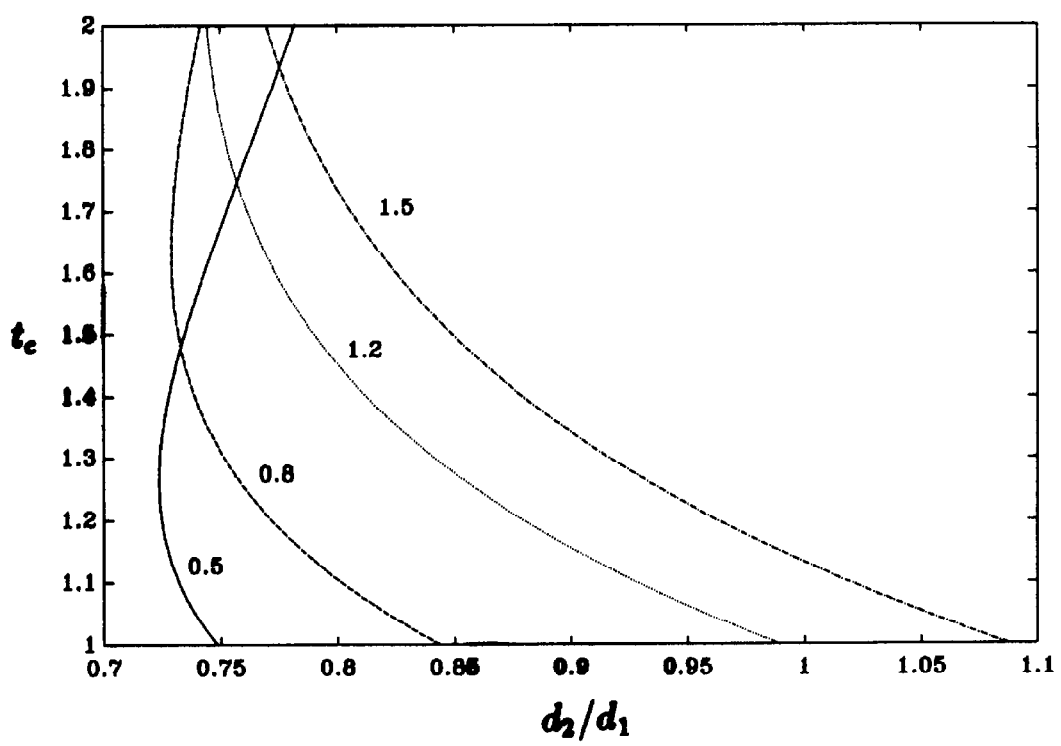

Fig. 10. Critical ratio d_2/d_1 versus t_c for different values of T.

of the critical visibility based on the two point formula, d_2, by the critical visibility based on the one point formula, d_1, versus t_c, and for different values of T. It can be seen that the ratio d_2/d_1 is, in general, less than one and that it exceeds the value of one for higher values of t_c as T increased.

Although use of the two point formula (64) provides a wider domain of linear stability, its effect on the nature of Hopf bifurcations must still be assessed. To this end we can write the control law (42) in the form,

$$\delta = k_1\psi + k_2 v + k_3 r + k_1 \tan^{-1} \frac{2y(t - T) - y(t - 2T)}{d}, \tag{65}$$

where we utilized the new navigational law (64). Consistent with our analysis so far, we expand (65) in a third order Taylor series using a first order expansion for $y(t - T)$ and $y(t - 2T)$. This procedure yields,

$$\delta = k_1\psi + k_2 v + k_3 r + \frac{k_1}{d} y - \frac{k_1}{3d^3} y^3. \tag{66}$$

We can see that the effect of the two point formula is to eliminate T from the third order Taylor series expansions. Based on the results presented in Section 4.3, this has an adverse effect on limit cycle stability. It should be recalled that higher values of T helped in establishing supercritical Hopf bifurcations. Therefore in the present case subcritical bifurcations will occur over a larger range of t_c. The physical explanation of this fact is that since now a more accurate navigational law is employed, the control law needs to be softer. Naturally, using three positional estimates, $y(t - T)$, $y(t - 2T)$, and $y(t - 3T)$ would have similar effects. The advantage of increased stability region, though, is not worth the additional computational effort.

6. Concluding remarks

A methodology for analyzing positional information time lags in the control law for vehicle maneuvering in the horizontal plane has been presented. The relationship of the critical visibility, control time constant, and time lag was established. Time lags have been approximated by first, second, and third order Taylor expansions. It was found that the first order approximation was the most conservative for controller design purposes since it predicted the highest required critical visibility distance. Frequency response techniques based on Nyquist's stability criterion virtually matched the third order Taylor approximations. The differences among the three approximations became more pronounced with increasing time lag and decreasing controller time constant.

Further analysis was conducted to characterize the stability results for any value of time lag using a normalization procedure and the first order approximation for time lag. This provides a quick design estimate for stability degredation which is valid regardless of vehicle characteristics.

A detailed Hopf bifurcation study demonstrated the mechanism of loss of stability through subcritical or supercritical bifurcations. Supercritical bifurcations were ensured for values of control time constant greater than a certain critical value. This critical value is decreasing for increasing rudder saturation limits and navigational time lag. The use of a two stage memory model was found to increase, in general, the region of linear stability but decrease the region of supercritical Hopf bifurcations.

7. Acknowledgements

The author would like to recognize the financial support of the Naval Postgraduate School Direct Research Fund.

8. References

[1] Bahrke, F. 'On-line Identification of the Speed, Steering and Diving Response Parameters of an Autonomous Underwater Vehicle from Experimental Data', Mechanical Engineer's Thesis, Naval Postgraduate School, Monterey, California, 1992.

[2] Chow, S.-N. and Mallet-Paret, J., 'Integral Averaging and Bifurcation', Journal of Differential Equations, 26, 1977, pp 112-159.

[3] Cottle, D.J., 'Mine Avoidance and Localization for Underwater Vehicles Using Continuous Curvature Path Generation and Non-linear Tracking Control', Mechanical Engineer's Thesis, Naval Postgraduate School, Monterey, California., 1993

[4] Friedland, B, 'Control System Design: An Introduction to State-Space Methods' (McGraw-Hill, New York), 1986.

[5] Guckenheimer, J. and Holmes, P., 'Nonlinear Oscillations, Dynamical Systems, and Bifurcations of Vector Fields' (Springer-Verlag, New York), 1983.

[6] Hassard, B. and Wan, Y.H., 'Bifurcartion Formulae Derived from Center Manifold Theory', Journal of Mathematical Analysis and Applications, 63, 1978, pp 297-312.

[7] Healey, A.J., McGhee, R.B., Cristi, R., Papoulias, F.A., Kwak, S.H., Kanayama, Y., Lee, Y., Shukla, S. and Zaky, A, 'Research on Autonomous Underwater Vehicles at the Naval Postgraduate School', Naval Research Reviews, XLIV, 1, 1992.

[8] Kanayama, Y. and Hartman, B.I., 'Smooth Local Path Planning for Autonomous Vehicles', Proceedings, IEEE International Conference on Robotics and Automation, Scottsdale, Arizona, 1989.
[9] Kwak, S.H., McKeon, J.B., Clynch, J.R. and McGhee, R.B., 'Incorporation of Global Positioning System into Autonomous Underwater Vehicle Navigation', Proceedings, IEEE Autonomous Underwater Vehicle Conference, Washington, D.C., 1992.
[10] Papoulias, F.A., 'Bifurcation Analysis of Line of Sight Vehicle Guidance Using Sliding Modes', International Journal of Bifurcation and Chaos, 1, 4, 1991.
[11] Papoulias, F.A., 'Guidance and Control Laws for Vehicle Path Keeping Along Curved Trajectories', Applied Ocean Research, 14, 1992, pp 291-302.
[12] Papoulias, F.A., 'Dynamics and Bifurcations of Pursuit Guidance for Vehicle Path Keeping in the Dive Plane', Journal of Ship Research, 37, 2, 1993.
[13] Papoulias, F.A. and Chism, S.R., 'Path Keeping of Autonomous Underwater Vehicles Using Sliding Mode Control', International Shipbuilding Progress, 39, 419, 1992.

9. Appendix

9.1. Elements of matrix $A_{ij,1}$

The entries of the eigenvalue problem (20) are given by,

$$A_{21,1} = b_1 u^2 \frac{k_1}{d} (d - uT),$$

$$A_{22,1} = a_{11} u + b_1 u^2 \left(k_2 - \frac{k_1}{d} T \right),$$

$$A_{23,1} = a_{12} u + b_1 u^2 k_3,$$

$$A_{24,1} = b_1 u^2 \frac{k_1}{d},$$

$$A_{31,1} = b_2 u^2 \frac{k_1}{d} (d - uT),$$

$$A_{32,1} = a_{21} u + b_2 u^2 \left(k_2 - \frac{k_1}{d} T \right),$$

$$A_{33,1} = a_{22}u + b_2u^2k_3,$$

$$A_{34,1} = b_2u^2 \frac{k_1}{d} .$$

9.2. Elements of matrix $A_{ij,2}$

The entries of the eigenvalue problem (22) are given by,

$$A_{21,2} = \frac{b_1u^2k_1d - b_1u^3k_1T}{d - 0.5b_1u^2k_1T^2} ,$$

$$A_{22,2} = \frac{a_{11}ud + b_1u^2k_2d - b_1u^2k_1T}{d - 0.5b_1u^2k_1T^2} ,$$

$$A_{23,2} = \frac{a_{12}ud + b_1u^2k_3d + 0.5b_1u^3k_1T^2}{d - 0.5b_1u^2k_1T^2} ,$$

$$A_{24,2} = \frac{b_1u^2k_1}{d - 0.5b_1u^2k_1T^2} ,$$

$$A_{31,2} = b_2u^2k_1d - b_2u^3k_1T + 0.5b_2u^2k_1T^2 \cdot \frac{b_1u^2k_1d - b_1u^3k_1T}{d - 0.5b_1u^2k_1T^2} ,$$

$$A_{32,2} = a_{21}ud + b_2u^2k_2d - b_2u^2k_1T + 0.5b_2u^2k_1T^2 \cdot \frac{a_{11}ud + b_1u^2k_2d - b_1u^2k_1T}{d - 0.5b_1u^2k_1T^2} ,$$

$$A_{33,2} = a_{22}ud + b_2u^2k_3d + 0.5b_2u^3k_1T^2 + 0.5b_2u^2k_1T^2$$

$$\times \frac{a_{12}ud + b_1u^2k_3d + 0.5b_1u^3k_1T^2}{d - 0.5b_1u^2k_1T^2} ,$$

$$A_{34,2} = b_2u^2k_1 + 0.5b_2u^2k_1T^2 \cdot \frac{b_1u^2k_1}{d - 0.5b_1u^2k_1T^2} .$$

9.3. Elements of matrices $A_{ij,3}$ and $B_{ij,3}$

The entries of the generalized eigenvalue problem (24) are given by,

$$B_{33} = b_1 u^3 \frac{k_1}{6d} T^3,$$

$$B_{35} = b_1 u^2 \frac{k_1}{6d} T^3,$$

$$B_{53} = 1 + b_2 u^3 \frac{k_1}{6d} T^3,$$

$$B_{55} = b_2 u^2 \frac{k_1}{6d} T^3,$$

$$A_{31} = b_1 u^2 k_1 - b_1 u^3 \frac{d}{k_1} T,$$

$$A_{32} = a_{11} u + b_1 u^2 k_2 - b_1 u^2 \frac{k_1}{d} T,$$

$$A_{33} = a_{12} u + b_1 u^2 k_3 + b_1 u^3 \frac{k_1}{2d} T^2,$$

$$A_{34} = b_1 u^2 \frac{k_1}{d},$$

$$A_{35} = b_1 u^2 \frac{k_1}{2d} T^2 - 1,$$

$$A_{51} = b_2 k_1 - b_2 u^3 \frac{k_1}{d} T,$$

$$A_{52} = a_{21} u + b_2 u^2 k_2 - b_2 u^2 \frac{k_1}{d} T,$$

$$A_{53} = a_{22} u + b_2 u^2 k_3 + b_2 u^3 \frac{k_1}{2d} T^2,$$

$$A_{54} = b_2 u^2 \frac{k_1}{d},$$

$$A_{55} = b_2 u^2 \frac{k_1}{2d} T^2 - 1.$$

9.4. Nonlinear expansion coefficients r_{ij}

The nonlinear expansion coefficients r_{ij} that are utilized in the definition of the cubic stability coefficient K are given by the following:

$$r_{11} = n_{12}l_{21} + n_{13}l_{31} + n_{14}l_{41},$$

$$r_{13} = n_{12}l_{23} + n_{13}l_{33} + n_{14}l_{43},$$

$$r_{22} = n_{22}l_{22} + n_{23}l_{32} + n_{24}l_{42},$$

$$r_{24} = n_{22}l_{24} + n_{23}l_{34} + n_{24}l_{44},$$

where we denote,

$$\mathbf{T} = [m_{ij}], \quad \mathbf{T}^{-1} = [n_{ij}], \qquad i, j = 1, \ldots, 4$$

For numerical purposes the critical eigenvector of **T** must be normalized so that its first nonvanishing coefficient is identically equal to 1. The coefficient l_{ij} are given by,

$$\begin{aligned}
\frac{l_{21}}{b_1u^2} = {} & \delta_{\psi\psi v}m_{11}^2m_{21} + \delta_{\psi vv}m_{11}m_{21}^2 + \delta_{\psi\psi r}m_{11}^2m_{31} + \delta_{\psi rr}m_{11}m_{31}^2 \\
& + \delta_{\psi\psi y}m_{11}^2m_{41} + \delta_{\psi yy}m_{11}m_{41}^2 + \delta_{vvr}m_{21}^2m_{31} + \delta_{vrr}m_{21}m_{31}^2 \\
& + \delta_{vvy}m_{21}^2m_{41} + \delta_{vyy}m_{21}m_{41}^2 + \delta_{rry}m_{31}^2m_{41} + \delta_{ryy}m_{31}m_{41}^2 \\
& + \delta_{\psi vr}m_{11}m_{21}m_{31} + \delta_{\psi vy}m_{11}m_{21}m_{41} + \delta_{\psi ry}m_{11}m_{41}m_{31} + \delta_{vry}m_{21}m_{41}m_{31} \\
& + \delta_{\psi\psi\psi}m_{11}^3 + \delta_{vvv}m_{21}^3 + \delta_{rrr}m_{21}^3 + \delta_{yyy}m_{41}^3,
\end{aligned}$$

$$\begin{aligned}
\frac{l_{22}}{b_1u^2} = {} & \delta_{\psi\psi v}(m_{11}^2m_{22} + 2m_{11}m_{12}m_{21}) + \delta_{\psi vv}(m_{12}m_{21}^2 + 2m_{11}m_{12}m_{22}) \\
& + \delta_{\psi\psi r}(m_{11}^2m_{32} + 2m_{11}m_{12}m_{31}) + \delta_{\psi rr}(m_{12}m_{31}^2 + 2m_{11}m_{31}m_{32}) \\
& + \delta_{\psi\psi y}(m_{11}^2m_{42} + 2m_{11}m_{12}m_{41}) + \delta_{\psi yy}(m_{41}^2m_{12} + 2m_{11}m_{41}m_{42}) \\
& + \delta_{vvr}(m_{21}^2m_{32} + 2m_{31}m_{21}m_{22}) + \delta_{vrr}(m_{22}m_{31}^2 + 2m_{31}m_{32}m_{21}) \\
& + \delta_{vvy}(m_{21}^2m_{42} + 2m_{41}m_{21}m_{22}) + \delta_{vyy}(m_{22}m_{41}^2 + 2m_{41}m_{42}m_{21}) \\
& + \delta_{rry}(m_{31}^2m_{42} + 2m_{41}m_{31}m_{32}) + \delta_{ryy}(m_{32}m_{41}^2 + 2m_{41}m_{42}m_{31}) \\
& + \delta_{\psi vr}[m_{11}m_{21}m_{32} + m_{31}(m_{11}m_{22} + m_{12}m_{21})] \\
& + \delta_{\psi vy}[m_{11}m_{21}m_{42} + m_{41}(m_{11}m_{22} + m_{12}m_{21})]
\end{aligned}$$

$$+ \delta_{\psi ry}[m_{11}m_{41}m_{32} + m_{31}(m_{11}m_{42} + m_{12}m_{41})]$$
$$+ \delta_{vry}[m_{21}m_{41}m_{32} + m_{31}(m_{21}m_{42} + m_{22}m_{41})]$$
$$+ \delta_{\psi\psi\psi}(3m_{11}^2m_{12}) + \delta_{vvv}(3m_{21}^2m_{22}) + \delta_{rrr}(3m_{31}^2m_{32}) + \delta_{yyy}(3m_{41}^2m_{42}),$$

$$\frac{l_{23}}{b_1u^2} = \delta_{\psi\psi v}(m_{11}^2m_{21} + 2m_{11}m_{12}m_{22}) + \delta_{\psi vv}(m_{11}m_{22}^2 + 2m_{12}m_{21}m_{22})$$
$$+ \delta_{\psi\psi r}(m_{12}^2m_{31} + 2m_{11}m_{12}m_{32}) + \delta_{\psi rr}(m_{11}m_{32}^2 + 2m_{12}m_{31}m_{32})$$
$$+ \delta_{\psi\psi y}(m_{12}^2m_{41} + 2m_{11}m_{12}m_{42}) + \delta_{\psi yy}(m_{42}^2m_{11} + 2m_{12}m_{41}m_{42})$$
$$+ \delta_{vvr}(m_{22}^2m_{31} + 2m_{21}m_{22}m_{32}) + \delta_{vrr}(m_{21}m_{32}^2 + 2m_{31}m_{22}m_{32})$$
$$+ \delta_{vvy}(m_{22}^2m_{41} + 2m_{21}m_{22}m_{42}) + \delta_{vyy}(m_{21}m_{42}^2 + 2m_{41}m_{42}m_{22})$$
$$+ \delta_{rry}(m_{32}^2m_{41} + 2m_{42}m_{31}m_{32}) + \delta_{ryy}(m_{31}m_{42}^2 + 2m_{41}m_{42}m_{32})$$
$$+ \delta_{\psi vr}[m_{12}m_{22}m_{31} + m_{32}(m_{11}m_{22} + m_{12}m_{21})]$$
$$+ \delta_{\psi vy}[m_{12}m_{22}m_{41} + m_{42}(m_{11}m_{22} + m_{12}m_{21})]$$
$$+ \delta_{\psi ry}[m_{12}m_{42}m_{31} + m_{32}(m_{11}m_{42} + m_{12}m_{41})]$$
$$+ \delta_{vry}[m_{22}m_{42}m_{31} + m_{32}(m_{21}m_{42} + m_{22}m_{41})]$$
$$+ \delta_{\psi\psi\psi}(3m_{11}m_{12}^2) + \delta_{vvv}(3m_{21}m_{22}^2) + \delta_{rrr}(3m_{31}m_{32}^2) + \delta_{yyy}(3m_{41}m_{42}^2),$$

$$\frac{l_{24}}{b_1u^2} = \delta_{\psi\psi v}m_{12}^2m_{22} + \delta_{\psi vv}m_{12}m_{22}^2 + \delta_{\psi\psi r}m_{12}^2m_{32} + \delta_{\psi rr}m_{12}m_{32}^2)$$
$$+ \delta_{\psi\psi y}m_{12}^2m_{42} + \delta_{\psi yy}m_{12}m_{42}^2 + \delta_{vvr}m_{32}^2m_{32} + \delta_{vrr}m_{22}m_{32}^2$$
$$+ \delta_{vvy}m_{22}^2m_{42} + \delta_{vyy}m_{22}m_{42}^2 + \delta_{rry}m_{32}^2m_{42} + \delta_{ryy}m_{32}m_{42}^2$$
$$+ \delta_{\psi vr}m_{12}m_{22}m_{32} + \delta_{\psi vy}m_{12}m_{22}m_{42} + \delta_{\psi ry}m_{12}m_{42}m_{32} + \delta_{vry}m_{22}m_{42}m_{32}$$
$$+ \delta_{\psi\psi\psi}m_{12}^3) + \delta_{vvv}m_{22}^3 + \delta_{rrr}m_{32}^3) + \delta_{yyy}m_{42}^3,$$

$$\frac{l_{31}}{b_2u^2} = \frac{l_{21}}{b_1u^2}$$

$$\frac{l_{32}}{b_2u^2} = \frac{l_{22}}{b_1u^2}$$

$$\frac{l_{33}}{b_2u^2} = \frac{l_{23}}{b_1u^2}$$

$$\frac{l_{34}}{b_2u^2} = \frac{l_{24}}{b_1u^2}$$

$$l_{41} \quad -\frac{1}{2}\, m_{11}^2\left(m_{21} + \frac{1}{2}\, u m_{11}\right),$$

$$l_{42} \quad -m_{11}\left(m_{12}m_{21} + \frac{1}{2}\, m_{11}m_{22} + \frac{1}{2}\, u m_{12}^2\right),$$

$$l_{44} \quad -m_{12}\left(m_{11}m_{22} + \frac{1}{2}\, m_{12}m_{21} + \frac{1}{2}\, u m_{12,11}\right),$$

$$l_{44} \quad -\frac{1}{2}\, m_{12}^2\left(m_{22} + \frac{1}{2}\, u m_{12}\right),$$

where the coefficients in a third order expansion of the control law are defined by

$$\delta_{\psi\psi v} = -\frac{1}{\delta_{sat}^2}\,(k_1')^2 k_2' + 0.5 k_1 \frac{T}{d_T} + \frac{k_1 T^3 u^3}{d_T^3},$$

$$\delta_{\psi vv} = -\frac{1}{\delta_{sat}^2}\, k_1'(k_2')^2 + \frac{u T^3 k_1}{d_T^3},$$

$$\delta_{\psi\psi r} = -\frac{1}{\delta_{sat}^2}\,(k_1')^2 k_3,$$

$$\delta_{\psi rr} = -\frac{1}{\delta_{sat}^2}\, k_1' k_3^2,$$

$$\delta_{\psi\psi y} = -\frac{1}{\delta_{sat}^2}\,(k_1')^2 \frac{k_1}{d_T} - \frac{T^2 u^2 k_1}{d_T^3},$$

$$\delta_{\psi yy} = -\frac{1}{\delta_{sat}^2}\, k_1' \frac{k_1^2}{d_T^2} + \frac{T u k_1}{d_T^3},$$

$$\delta_{vvr} = -\frac{1}{\delta_{sat}^2}\,(k_2')^2 k_3,$$

$$\delta_{vrr} = -\frac{1}{\delta_{sat}^2}\, k_2' k_3^2,$$

$$\delta_{vvy} = -\frac{1}{\delta_{sat}^2}\,(k_2')^2 \frac{k_1}{d_T} - \frac{k_1 T^2}{d_T^3},$$

$$\delta_{vyy} = -\frac{1}{\delta_{sat}^2}\, k_2' \frac{k_1^2}{d_T^2} + \frac{T k_1}{d_T^3},$$

$$\delta_{rry} = -\frac{1}{\delta_{sat}^2} k_3^2 \frac{k_1}{d_T},$$

$$\delta_{ryy} = -\frac{1}{\delta_{sat}^2} k_3 \frac{k_1^2}{d_T^2},$$

$$\delta_{\psi vr} = -\frac{1}{\delta_{sat}^2} 2k_1'k_2'k_3,$$

$$\delta_{\psi vy} = -\frac{1}{\delta_{sat}^2} 2k_1'k_2' \frac{k_1}{d_T} - 2\frac{T^2uk_1}{d_T^3},$$

$$\delta_{\psi ry} = -\frac{1}{\delta_{sat}^2} 2k_1'k_3 \frac{k_1}{d^t},$$

$$\delta_{vry} = -\frac{1}{\delta_{sat}^2} 2k_2'k_3 \frac{k_1}{d_T},$$

$$\delta_{\psi\psi\psi} = -\frac{1}{\delta_{sat}^2} \frac{1}{3} (k_1')^3 + \frac{k_1Tu}{6d_T} + \frac{k_1T^3u^3}{3d_T^3},$$

$$\delta_{vvv} = -\frac{1}{\delta_{sat}^2} \frac{1}{3} (k_2')^3 + \frac{k_1T^3}{3d_T^3},$$

$$\delta_{rrr} = -\frac{1}{\delta_{sat}^2} \frac{1}{3} k_3^3,$$

$$\delta_{yyy} = -\frac{1}{\delta_{sat}^2} \frac{1}{3} \frac{k_1^3}{d_T^3} - \frac{2k_1}{3d^3},$$

and

$$k_1' = k_1 - k_1 \frac{Tu}{d},$$

$$k_2'1 = k_2 - k_1 \frac{T}{d},$$